Mean free-air gravity anomalies in the mountains

Juraj Janák[(1)] and Petr Vaníček[(2)]

[1.] Department of Theoretical Geodesy, Slovak University of Technology,

Radlinského 11, 81368 Bratislava, Slovak Republic

janak@svf.stuba.sk

[2.] Department of Geodesy and Geomatics Engineering,

University of New Brunswick, GPO Box 4400, Fredericton, Canada

vanicek@unb.ca

Abstract

The mean free-air gravity anomalies are often needed in geodesy for gravity field modelling. Two possible ways of compiling the mean free-air gravity anomalies are discussed. One way is via simple Bouguer gravity anomalies and the second and more time consuming way is via refined Bouguer gravity anomalies. Theoretically the differences between using any of the two ways should not be significant. However, a numerical experiment conducted in one part of Rocky Mountains revealed large and systematic differences. The effect of these differences on the geoid model is more then two meters in the test area. Our investigation shows that this bias is caused by the location of gravity measurement points, chosen mostly on hill-tops. In such points the terrain correction to gravity is systematically larger than the mean value of the correction. Therefore it is not possible to prevent the mean free-air gravity anomalies obtained from simple Bouguer gravity anomalies from having a systematic bias. The more rigorous way of computing the mean free-air gravity anomalies is via refined Bouguer gravity anomalies.

Introduction

Points of observation for surface gravity mapping are usually chosen to be approximately evenly distributed over the whole area of interest. An approximate distance between the observed points stem from the prescribed number of points per squared kilometre. This is natural and logical requirement. In the mountains, however, it is often impossible to preserve this desideratum because of the terrain roughness and large inaccessible areas. Therefore, according to way of data collection, we can find

mountainous areas where observations are located systematically in the valleys or on the other hand on the tops of the hills. This systematic location of the observed gravity point can become a serious obstacle for correct compilation of the mean gravity anomalies. The question can arise here, why do we need the mean values instead of the originally measured point values? The answer is based on the fact that we don't know how to integrate the point values over the surface and usually for gravity field modeling the surface integrals must be solved. Therefore one should either approximate the point values using analytical function, e.g. splines, or compile the mean values. The usual way how to create the mean values from irregularly distributed measured values is to produce the regular grid using interpolation followed by averaging over chosen surface cells. In this paper we are focused on mean free-air gravity anomalies because they are, in a wider sense, the basis of both geoid and quasigeoid computation as well as for the determination of deflections of the vertical. The problem with the accuracy of the mean free-air gravity anomalies has been studied in earlier works, e.g. *(Moritz, 1964)* and to the same problem has been pointed out in *(Torge, 1989, p. 58)* mentioning so called representation error. The similar topic has been treated in some more recent papers, e.g. *(Featherstone and Kirby, 2000)* and *(Goos et al., 2003)* focused on Australian territory, where interestingly different results and conclusions have been obtained comparing with those obtained in our test.

The two ways of mean free-air gravity anomaly determination

Let us assume that we have gravity measurements (magnitude of the gravity vector) on the earth surface $g(r_b, \Omega)$ at horizontal locations $\Omega = (\varphi, \lambda)$ and let us suppose that these

values have been corrected for time dependent effects, such as tides. From these values it is easy to compute the point values of free-air gravity anomalies at the same locations using the formula *(Torge, 1989, Eq. (3.7a))*

$$\Delta g^{FA}(r_t,\Omega) = g(r_t,\Omega) - \gamma_0(r_e,\Omega) + \delta g^{FA}(\Omega), \qquad (1)$$

where $g(r_t, \Omega)$ is the measured gravity on the topography, $\gamma_0(r_e, \Omega)$ is the normal gravity on the reference ellipsoid. The term $\delta g^{FA}(\Omega)$ denotes the free-air reduction of normal gravity defined by the following expression

$$\delta g^{FA}(\Omega) \cong -\left[\frac{\partial \gamma_0(r_e,\Omega)}{\partial h} H_N(\Omega) + \frac{1}{2}\frac{\partial^2 \gamma_0(r_e,\Omega)}{\partial h^2} H_N^2(\Omega) + \frac{1}{6}\frac{\partial^3 \gamma_0(r_e,\Omega)}{\partial h^3} H_N^3(\Omega)\right], \qquad (2)$$

where H_N stands for normal height. Because of the correlation of free-air anomalies with heights, the roughness of the free-air gravity anomalies is similar to the roughness of the terrain. Therefore, in the mountains it is not possible to interpolate and average these anomalies directly, unless we have really dense gravity mapping (e.g. 10 values per km^2) which is usually not the case. Thus in order to minimise the interpolation error we have to follow one of two possible ways showed in Fig.1.

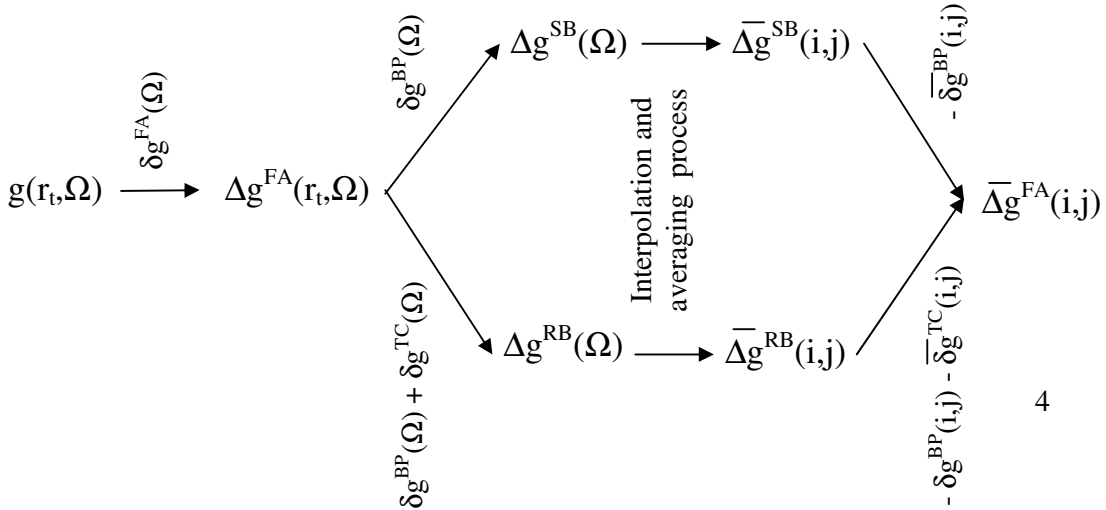

Fig. 1: Two ways of mean free-air gravity anomaly determination.

We can either use

1) the simple Bouguer gravity anomalies Δg^{SB}, related to free-air anomalies by the following formula *(Heiskanen and Moritz, 1967, Eq. (3-18))*:

$$\Delta g^{SB}(\Omega) = \Delta g^{FA}(r_t, \Omega) + \delta g^{BP}(\Omega), \quad (3)$$

where δg^{BP} denotes the Bouguer plate reduction *(ibid., Eq. (3-15))*

$$\delta g^{BP}(\Omega) = -2\pi G \rho H(\Omega), \quad (4)$$

G stands for the Newton gravitation constant and ρ represents the volume density of topographical masses. As the second and more laborious choice we can use

2) the refined Bouguer gravity anomalies Δg^{RB}, related to free-air anomalies by *(ibid., Eq. (3-21))*

$$\Delta g^{RB}(\Omega) = \Delta g^{FA}(r_t, \Omega) + \delta g^{BP}(\Omega) + \delta g^{TC}(\Omega), \quad (5)$$

which differ from the simple Bouguer anomalies by the point terrain correction $\delta g^{TC}(\Omega)$. Both, the simple and the refined Bouguer gravity anomaly fields are smooth enough to perform an interpolation and averaging operations over the point values within a specific geographical cell and obtain the corresponding mean values on a regular grid.

Each grid node is located in the centre of the corresponding cell and the value represents the mean value for that particular cell.

Now we can close the loop in Fig.1 by computing the two sets of mean free-air gravity anomalies both ways. We expected both sets to be similar, meaning that the differences between them should be randomly distributed around zero and their values should be within a reasonable confidence interval. We decided to check this numerically in one part of Rocky Mountains.

The Rocky Mountains Experiment

The biggest problem in the geoid determination is encountered in the mountains. Therefore the area in the Rocky Mountains, delimited by parallels 40°N and 66°N, and meridians 210°E and 252°E, was chosen for our test. For this region we obtained the surface and marine gravity data from Geodetic Survey Division, Natural Resources Canada, in Ottawa. In Fig.2 we show the distribution of more than 300,000 gravity points over the area. The average number of gravity points per one degree squared is about 300 and the average distance between gravity stations is approximately 6 km. Several digital elevation models (DEM) were used for the calculation of the terrain effect: the Canadian Digital Elevation Data (CDED) 3″ by 3″ in Alberta, Yukon and Northwest Territories; the provincial DEM 1″ by 1″ in British Columbia; NGSDEM99 1″ by 1″ in the US part of the area and 30″ by 30″ mean heights for Alaska. All mentioned data sets are compatible in sense of vertical datum. The topography of the region of interest can be seen in Fig.3.

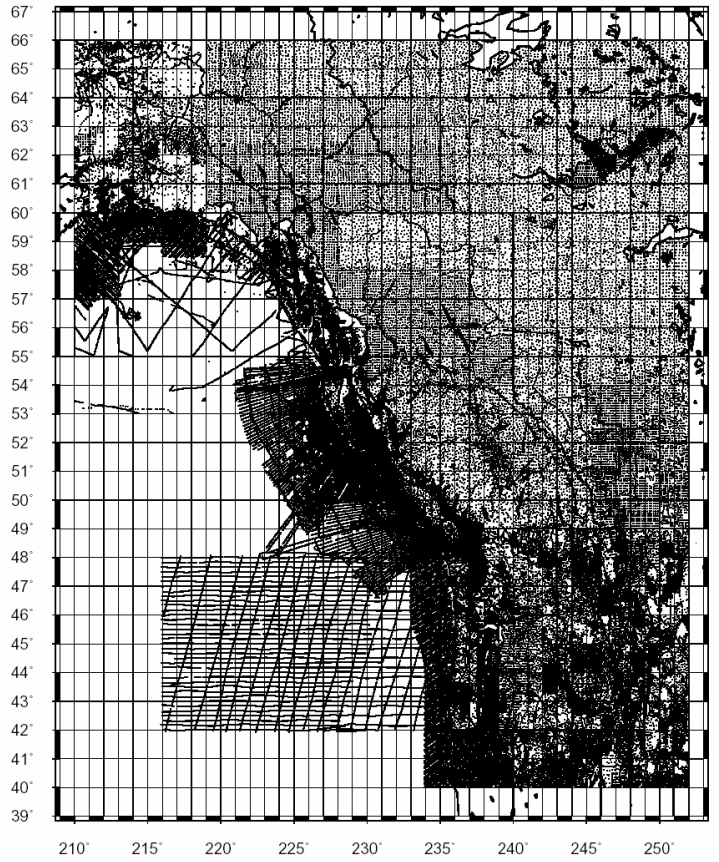

Fig. 2: Distribution of the measured gravity points.

The values of free-air gravity anomalies obtained at the observation points from Eq. (1) served as the input into our numerical test. Following the two ways shown in Fig. 1, two sets of mean free-air gravity anomalies were obtained. The differences between the two sets were computed and the results are displayed in Fig.4. Minimum, maximum and mean differences are stored in Tab.1. In order to obtain the approximate effect of these differences on the geoid, the Stokes integration within a 6° spherical cap was performed. The effect on the geoid, after cutting out the edge affected areas, is shown in Fig.5.

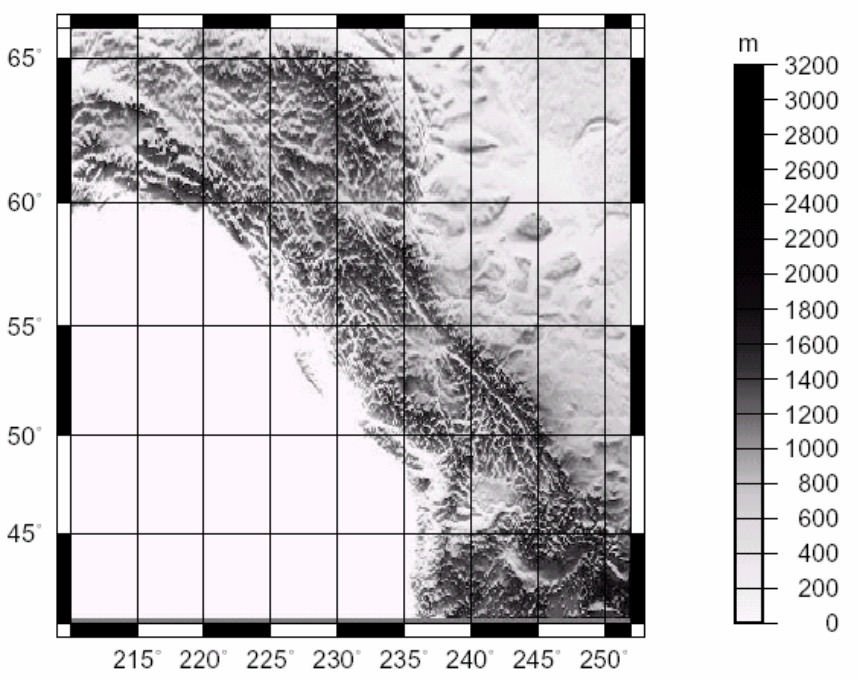

Figure 3: Topography in the region of interest.

Minimum, maximum and mean values are shown in Tab.1. The effect appears to be surprisingly systematic and quite large. It demonstrates that computing mean free-air gravity anomalies via refined Bouguer anomalies instead of simple Bouguer anomalies in the Rocky Mountains, we obtain a geoid model which is, in some places, higher by more then 2 meters.

File	$\overline{\Delta g_1}^{FA}$	$\overline{\Delta g_2}^{FA}$	$\overline{\Delta g_2}^{FA} - \overline{\Delta g_1}^{FA}$	ΔN
Units	mgal	mgal	mgal	m
Area	A	A	A	B
Min.	-167.68	-167.72	-35.64	-0.25
Max.	328.12	296.44	35.35	2.29
Mean	2.20	2.81	0.61	0.47

Tab. 1: Basic statistics of the investigated files. $\overline{\Delta g_1}^{FA}$ are the mean free-air gravity anomalies 5′ by 5′ computed via simple Bouguer graviy anomalies, $\overline{\Delta g_2}^{FA}$ are the mean free-air gravity anomalies 5′ by 5′ computed via refined Bouguer graviy anomalies and ΔN are the differences between the meen free-air gravity anomalies after Stokes's integration up to 6° spherical radius that gives us an approximate effect on the geoid. Area A is bounded by parallels and meridians: 40°N < φ < 66°N, 210°E < λ < 252°E. Area B is smaller to avoid the edge effect: 46°N < φ < 60°N, 222°E < λ < 246°E.

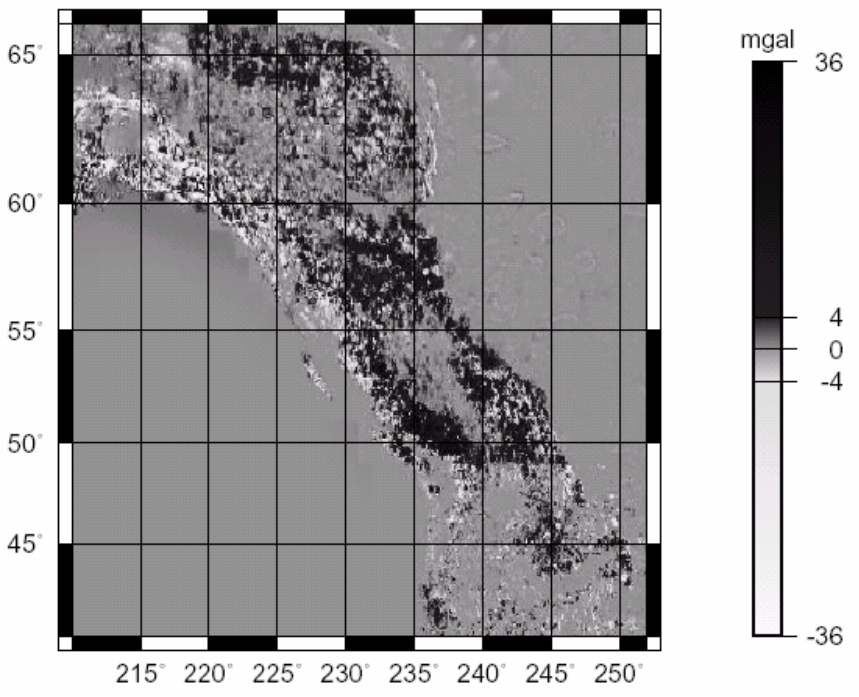

Figure 4: Differences between two sets of the free-air gravity anomalies.

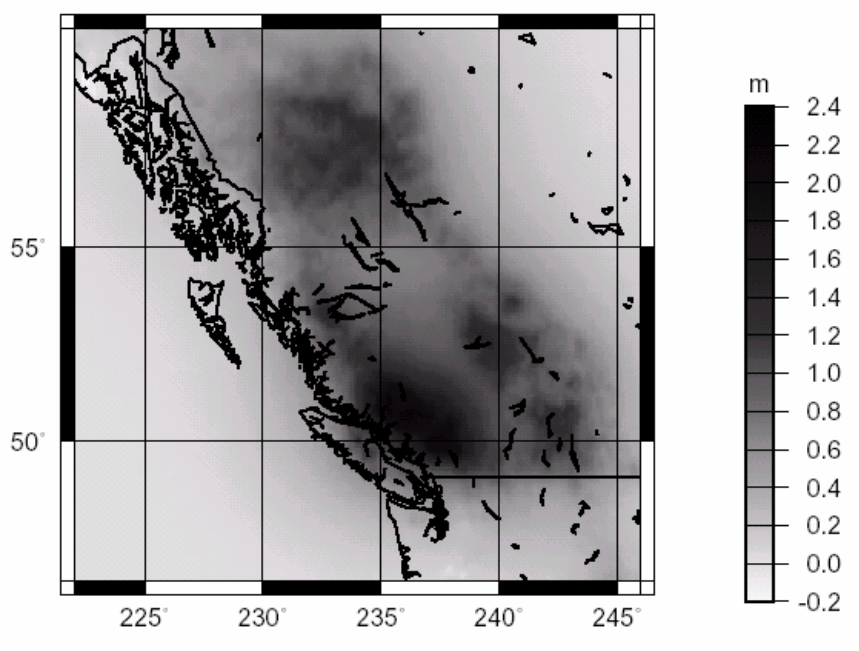

Figure 5: Effect of the free-air gravity anomalies difference on the geoid.

The basic questions now arise: What is the origin of this significant systematic influence and which one of the two discussed approaches is more rigorous. In order to find the answer to these questions we focused more closely on one 6° by 6° sub-area delimited by parallels 52°N and 58°N, and meridians 232°E and 238°E. The topography of this sub-area is plotted in Fig.6. The quantity we wish to discuss in particular, is the terrain correction. First, the terrain correction was computed at each and every one of the 3201 observation points and then the same quantity was computed on a regular geographic grid of 30″ by 30″ in the whole sub-area (518400 grid nodes). In both cases, the terrain correction was computed using the spherical model (Martinec and Vaníček, 1994), integrated within a 3° spherical cap by means of the analytical expression for the integration kernel derived by *(Martinec, 1998).*

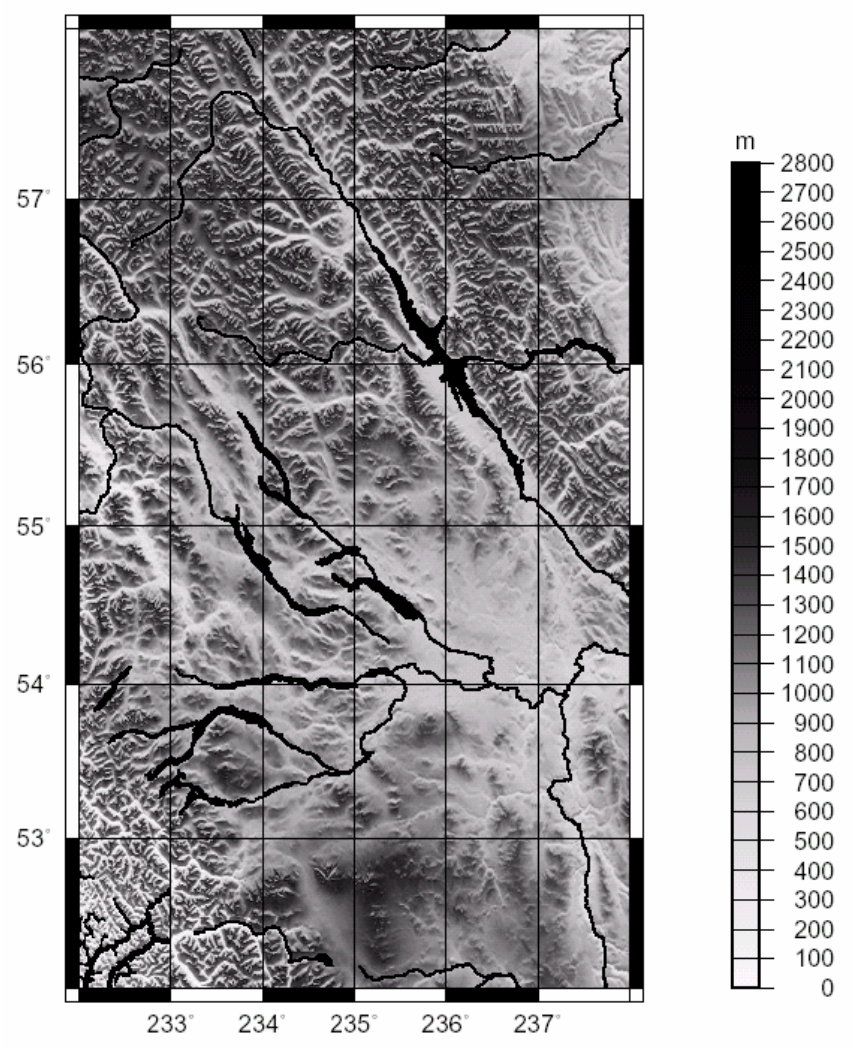

Figure 6: Topography in the 6° × 6° sub-area.

The simple averages of terrain correction for 1° by 1° cells were evaluated from the values computed at the observation points as well as from the values computed on a regular grid. This was done for all 36 cells of 1° by 1° as it is shown in Fig.7. Interestingly, the average terrain corrections obtained from observation points are larger in every 1° by 1° cell with the exception of 3 relatively flat cells. Clearly, the average

terrain correction obtained from the regular grid is more realistic because it is obtained from more then 100 times larger amount of uniformly distributed points.

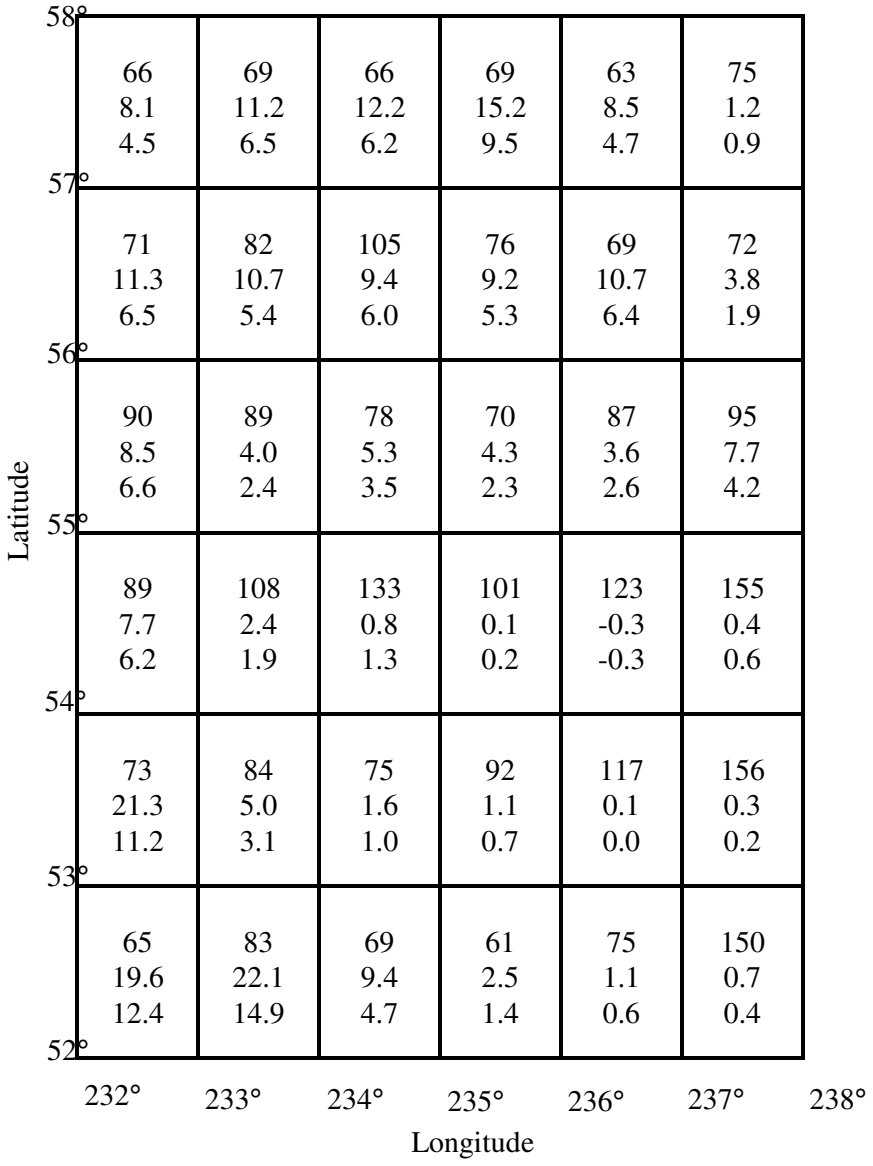

Figure 7: Average terrain corrections for 1°×1° cells. Each cell contain the following numbers (from the top): number of the observed gravity points, average terrain correction computed at the observed gravity points in mgal, average terrain correction computed at the 14400 regularly distributed points in mgal.

After noting these results, a more detailed analysis of the location of the observation points was done. One example of such detailed analysis is shown in Fig.8, where one particular observation point is located at the local terrain maximum; it is shown together with the terrain correction for the area. It can be seen that at the observation point the terrain correction grows up very steeply. Other gravity observation points display similar characteristics.

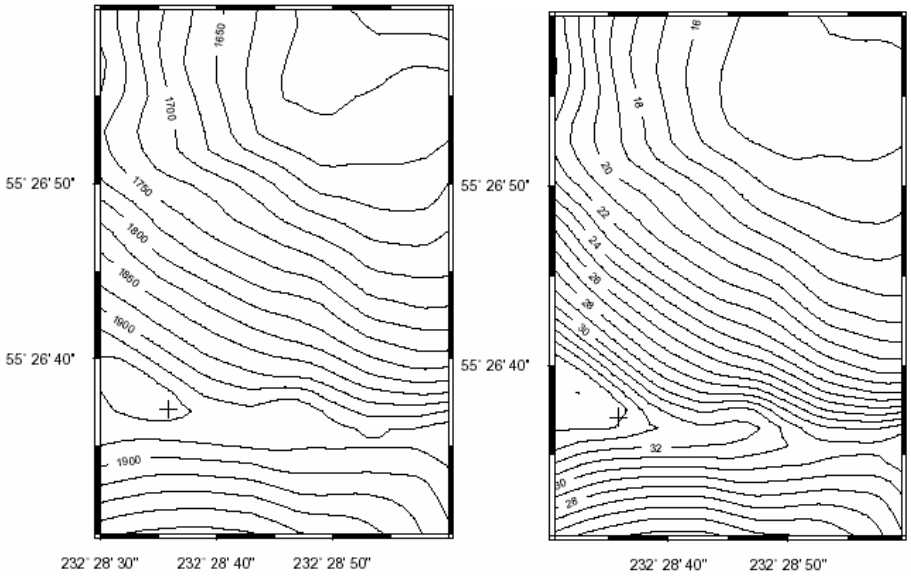

Figure 8: Topography (left) and terrain correction (right) in the vicinity of a particular observed gravity point. Units are *m* for topography and *mgal* for terrain correction.

In order to show the dependence between the elevation and the terrain correction mathematically, let us focus on a radial derivative within the radial integral of the Newton kernel $\tilde{L}(r,\psi,r') = \int_{r'} \frac{r'^2}{L(r,\psi,r')} dr'$ as it is evaluated analytically by Martinec *(1998, Eq. (3.54))*

$$\frac{\partial \tilde{L}^{-1}(r,\psi,r')}{\partial r} = \left[\left(r'^2 + 3r^2\right)\cos\psi + \left(1 - 6\cos^2\psi\right)rr'\right]L^{-1}(r,\psi,r') + \\ + r\left(3\cos^2\psi - 1\right)\ln\left|r' - r\cos\psi + L(r,\psi,r')\right|. \qquad (6)$$

In Eq. (6) r and r' are the radial distances of the computation point and integration element respectively, ψ is their spherical and L is their spatial distance. Eq. (6) represents the integration kernel for the evaluation of the effect of the topographical masses, i.e., masses between the geoid and earth surface, on gravity. Provided that the computation point is on the earth surface and after subtracting the effect of the spherical Bouguer shell we get the integration kernel for the spherical terrain correction in the following form

$$K(r,t,r') = r\left[\left(\left(\frac{r'}{r}\right)^2 + 3\right)t + \left(1 - 6t^2\right)\frac{r'}{r}\right]\left[\left(\frac{r'}{r}\right)^2 - 2t\frac{r'}{r} + 1\right]^{-\frac{1}{2}} - \\ - r\left(-6t^2 + 4t + 1\right)(2 - 2t)^{-\frac{1}{2}} + r\left(3t^2 - 1\right)\ln\frac{\frac{r'}{r} - t + \left[\left(\frac{r'}{r}\right)^2 - 2\frac{r'}{r}t + 1\right]^{\frac{1}{2}}}{1 - t + (2 - 2t)^{\frac{1}{2}}}, \qquad (7)$$

where $t=\cos\psi$. Using Eq. (7) we can investigate the correlation between the terrain correction and the elevation difference $\Delta H=H'-H$, where $H'=r'-R$, $H=r-R$ and R is the radius of the sphere used in the spherical model. Figs. 9 and 10 show such a correlation for an integration element located at the spherical distance ψ=0.01° (approximately 1km) and ψ=0.001° (approximately 0.1km) respectively for realistic range of ΔH. As it

can be seen from the graphs (Figs. 9 and 10), in the first approximation, the integration kernel *K* is a quadratic function of height.

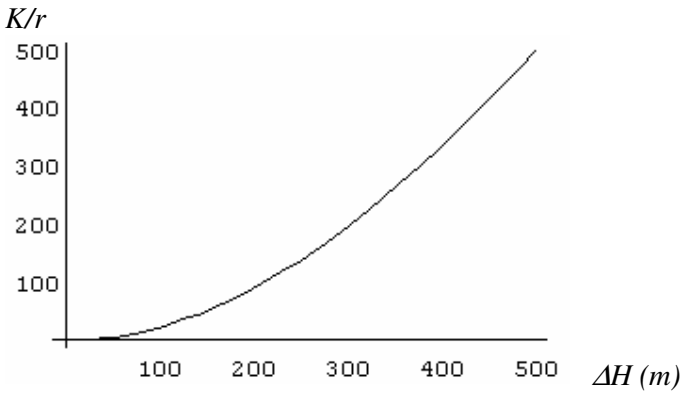

Figure 9: Integration kernel for terrain correction $K(r,\psi,r')/r$ for $\psi = 0.01°$ ($\approx$1100m), $r = 6378200m$ and $r' \in \langle 6378200m, 6378700m \rangle$, where $\Delta H = r' - r$.

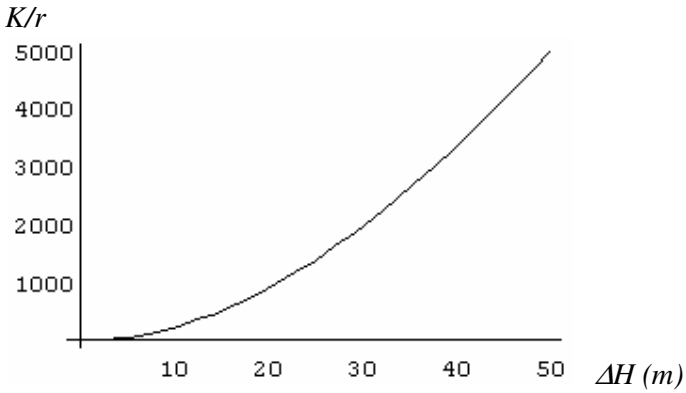

Figure 10: Integration kernel for terrain correction $K(r,\psi,r')/r$ for $\psi = 0.001°$ ($\approx$ 110m), $r = 6378200m$ and $r' \in \langle 6378200m, 6378250m \rangle$, where $\Delta H = r' - r$.

In fact if we have more points that behave as the one shown in Fig.8, the simple Bouguer gravity anomaly becomes systematically affected and it is not possible to interpolate with any reasonable accuracy. Our investigation in the Rocky Mountains,

especially in the area shown in Fig.7, confirmed that a significant number of observed gravity points in the Rocky Mountains are located at or in the vicinity of the local terrain maxima. As a consequence, the mean free-air anomalies as well as the geoid model computed via simple Bouguer gravity anomalies are systematically affected for more then 20 mGals and 2 meters respectively, as it is shown in Figs.4 and 5.

Conclusions

The answer to the first question we posed above is: The origin of the systematic discrepancy between the two sets of mean free-air gravity anomalies is in the location of the observation points. Too many gravity points in the Rocky Mountains are located at the local terrain tops, where the terrain correction is also extremely large. Therefore the simple Bouguer gravity anomalies computed at these points are too biased for a meaningful interpolation and averaging. The more rigorous and correct way of the compilation of the mean free-air gravity anomalies is via refined Bouguer gravity anomalies. This, of course, is more time consuming because it requires the evaluation of the terrain correction both at the observation points and, after the interpolation and averaging, also on chosen regular grid in order to obtain the mean terrain correction with sufficient accuracy.

Acknowledgement

We want to thank all who supported our research related to this paper, especially: The GEOIDE Centre of Excellence, Geodetic Survey Division (GSD) in Ottawa, Government of the Province of British Columbia, the US National Imagery and Mapping Agency (NIMA) and NATO. We also wish to single out Pavel Novák and Bas Alberts for their help with the software and computation.

References

Featherstone, W.E. and J.F. Kirby. 2000. The reduction of aliasing in gravity observations using digital terrain data and its effect upon geoid computaion. Geophysical Journal International, 141(1), pp. 204-212.

Goos, J.M., Featherstone, W.E., Kirby, J.F. and S.A. Holmes. 2003. Experiments with two different approaches to gridding terrestrial gravity anomalies and their effect on regional geoid computation. Survey Review, Vol. 37, No. 288, pp.

Heiskanen, W.A. and H. Moritz. 1967. *Physical Geodesy*, W.H. Freeman and Co., San Francisco and London.

Martinec, Z. and P. Vaníček. 1994. Direct topographical effect of Helmert's condensation for a spherical approximation of the geoid. *Manuscripta Geodaetica, 19*, pp. 257-268.

Martinec, Z. 1998. *Boundary-Value Problems for Gravimetric Determination of a Precise Geoid.* Springer-Verlag, Berlin, Heidelberg, New York.

Moritz, H. 1964. Accuracy of mean gravity anomalies obtained from point and profile measurements. Public. Isostat. Inst. Int. Assoc. Geod., No. 45, Helsinky.

Torge, W. 1989. Gravimetry. De Gruyter, Berlin.